NASA Technical Memorandum 83331

The Thermal Fatigue Resistance of H-13 Die Steel for Aluminum Die Casting Dies

Betty J. Barrow
Lewis Research Center
Cleveland, Ohio

Prepared for the
Let's Do It Ourselves: In Science and Technology
sponsored by the National Technical Association
Baltimore, Maryland, August 2-7, 1982

NASA

THE THERMAL FATIGUE RESISTANCE OF H-13 DIE STEEL FOR ALUMINUM DIE CASTING DIES

LEWIS RESEARCH CENTER
CLEVELAND, OH

AUGUST 82

THE THERMAL FATIGUE RESISTANCE OF H-13 DIE STEEL FOR ALUMINUM DIE CASTING DIES

Betty J. Barrow

National Aeronautics and Space Administration
Lewis Research Center
Cleveland, Ohio 44135

ABSTRACT

This investigation was conducted to determine the effects of welding, selected surface coatings and stress relieving on the thermal fatigue resistance of H-13 Die Steel for aluminum die casting dies.

Eleven thermal fatigue specimens were utilized in this investigation and are categorized as follows: control, stress relieved, welded, and surface treated (five different surface treatments were evaluated). Stress relieving was conducted after each 5000 cycle interval at 1050° F for 3 hours. Four thermal fatigue specimens were welded with H-13 or maraging steel welding rods at ambient and elevated temperatures and subsequently, subjected to different post-weld heat treatments. The surface treatments used are proprietary but are described in generic terms. Crack patterns were examined at 5000, 10 000, and 15 000 cycles. The thermal fatigue resistance is expressed by two crack parameters which are the average maximum crack and the average cracked area.

The results indicated that a significant improvement in thermal fatigue resistance over the control was obtained from the stress-relieving treatment. Small improvements in thermal fatigue resistance were obtained from the H-13 welded specimens and from a salt bath nitrogen and carbon-surface treatment which is attributed to the alleviation of the residual stresses and the formation of a diffusion layer at the surface. The other surface treatments and welded specimens either did not affect or had a detrimental influence on the thermal fatigue properties of the H-13 die steel.

INTRODUCTION

Stress, Erosion and Corrosion Effects

In die casting, the molten metal is forced into the mold or die under high velocity and pressures and held against the die wall until solidification occurs.[1] After the casting has cooled sufficiently, the die is opened and the part is ejected by pins which are mechanically activated. To increase the rate of cooling of the die and casting, the dies are usually water cooled.

Dies for aluminum alloys are significantly higher in cost than those for lower melting temperature alloys. Depending on its intricacy, the cost of the die may be more than the machinery required to operate it. Efforts to hold cost within reasonable limits must include increasing the production life of the die. Therefore, prevention of die failure can make a major contribution toward the profitability of the die casting operation.

Aluminum die casting dies are subjected to high thermal-mechanical loads. As a result, the service life of these dies can be limited. The major causes of die failure are heat checking, cleavage or gross cracking, decarburization, erosion damage and indentations. Of these, the most frequent cause of die

failure is due to heat checking. Heat checking is caused by thermal fatigue which results from the rapidly alternating temperatures and thermal gradients normal to the die surface. These cyclical temperature fluctuations induce stress and strain combinations that can produce cracking of the material resulting in premature failure.[2] The magnitude of the thermal stresses and strains depend upon the mechanical and thermophysical properties of the material, cooling rates, and the maximum and minimum temperatures of the thermal cycle.[3]

Thermal fatigue cracks or heat checks initiate as pits at points of maximum stress and at inclusions or imperfections present on or near the specimen surface. In ductile materials such as H-13 die steel, cracking is preceded by surface markings that appear as small grooves. Heat checking occurs as a fine network of cracks located on the die surface. Propagation of these cracks is perpendicular to the die face. Heat checks are transgranular and appear straight and sharp with a greater thickness near the surface. Figure 1 is a photomicrograph of the control specimen at 50X (unetched) to show the appearance of a heat check on the die surface.

When molten liquid metal is injected into the cold die, the surface is immediately subjected to a severe temperature increase. This temperature is rapidly decreased by conduction of heat back into the underlying lower temperature die steel. The temperature variations at the die surface during a casting cycle are illustrated in figure 2.[4] The magnitude of this temperature fluctuation is determined by the heat transfer characteristics of the die surface due to the presence of coatings, oxide layers and dimensional configurations. The die surface in immediate contact with the molten metal expands and contracts continuously as the casting cycle is repeated, resulting in thermal stresses at the surface due to self-constraint. This continued sequence of alternating stresses can result in plastic deformation of the material. Under these conditions, the induced stresses are capable of exceeding the fatigue strength of the material leading to heat checks.

Both the initiation and propagation of thermal fatigue cracks are further influenced by corrosion. Throughout the operation of the die, it is exposed to an oxidizing atmosphere. Progressive oxidation occurs with additional cycling. As a result, corrosion pits which form are filled with oxides. The oxides present occupy a larger volume than the metal which they replaced, resulting in a wedging action and a tri-axial tensile stress state at the tip of the crack. These tri-axial tensile stresses are a major contributor to crack propagation.

The purpose of this investigation is to determine what effect selected surface treatments, various welding procedures, and stress-relieving has on the thermal fatigue resistance of H-13 die steel. A comparative study will determine which surface treatment and welding procedure has the most beneficial and most detrimental effect on the thermal fatigue properties of the H-13 die steel. Finally, a metallographic examination of the transverse cross-section of each corner will show the interaction of the surface treatments and welds with the base metal. This analysis is used to determine the relationship between the thermal fatigue properties and microstructures.

MATERIALS AND PROCEDURES

The selection of the appropriate base metal to use for die casting dies requires a consideration of its thermal fatigue resistance, toughness, hot hardness, machinability and cost. H-13 die steel is most widely used in the die casting industry because it offers the best compromise of this range of

material characteristics. Also, H-13 die steel possesses a low coefficient of thermal expansion and a high thermal conductivity which are essential for good thermal fatigue resistance. The optimum hardness level for the maximum thermal fatigue resistance in H-13 die steel is Rockwell C 46[5] (R_C). A hardness level over R_C46 lowers the toughness and can lead to gross cracking. If the hardness level is lower than R_C46, the H-13 die steel will become susceptible to heat checking and /or erosion.

The eleven thermal fatigue specimens utilized in this investigation were machined from a 3 1/2 inch diameter bar of H-13 die steel to meet the dimensions shown in figure 3 plus a 0.050 inch allowance for grinding after heat treatment to reduce surface decarburization. The composition of this steel can be seen in table 1. After machining, all specimens were austenitized at 1850° F for 2 hours in a salt bath and then oil quenched. Following the quench, the specimens were double tempered in salt at 1100° F for 1 hour and then air-cooled, the hardness at this time was 48-49 R_C, so the thermal fatigue test specimens were tempered at 1100° F for 7 1/2 hours in an air furnace. This lowered the hardness to the required value of R_C46.

In all specimens where a surface coating was to be applied, the two corners to be coated (alternate corners) were finished to final dimensions. The 0.050 inch stock was not removed from the other alternate corners which were to be used as the control. This 0.050 inch of stock which remained was removed as a last operation before testing to eliminate by-products of the coating treatment from the control corner surfaces.

The coatings tested were proprietary. The commercial designation of these coatings is not employed but each are described in generic terms. Coating A is a salt bath nitrogen and carbon diffused surface treatment. Coating A was applied at 1060° F for 2 hours. Coating B is a low temperature salt bath treatment. Coating C is a Boron diffusion surface treatment. This process tempered the steel; therefore, it was necessary to re-heat treat the specimen by austenitizing at 1950° F for 2 hours. The process was completed by a double-temper at 1100° F for 1 hour in order to maintain the hardness value of R_C46. Coatings D and E are nitrogen diffused surface treatments. Coating D was applied with an ionized gas at 986° F for 24 hours and Coating E was gas nitrided at 1000° F for 24 hours.

The specimen to be stress-relieved was heated to 1050° F for 3 hours and allowed to furnace cool to 800° F after every 5000 cycles. The specimen was then air-cooled to room temperature. The corners of the fatigue specimens to be welded were undercut along the entire length of the specimen a distance of 3/8 inch from the edge to a depth of 0.094 inch. All welds were applied with the gas shield metal ARC welding process (GMAW). The compositions of the maraging and H-13 welding rods are listed in table I. The weld temperature and post-weld heat treatments are listed in table II.

Metallographic examination of these weld areas indicated that the H-13 welds were made in six passes and the maraging steel in ten passes. The weld deposits were made sequentially with no waiting period to reach the specified welding temperature before depositing the next weld bead. This procedure undoubtedly resulted in higher interpass temperatures than the stated welding temperatures. The .010" radius was placed on all corners before the post-weld heat treatment.

A schematic diagram of the thermal fatigue test equipment is shown in figure 4. The function of this equipment was to simulate the environmental conditions indicative of die casting. The specimen was immersed into a molten 380 aluminum alloy bath at an average temperature of 1300° F for 13 seconds, followed by a 23 second cooling period in air at ambient temperatures.

The specimen was internally cooled by a continuous flow of water at a rate of 1 gallon per minute. To maintain the molten bath temperature of 1300° F, two chromel-alumel thermocouples were employed to monitor and record this temperature throughout cycling. Immediately prior to the immersion of the specimen into the bath, its surface was sprayed with a water-base die lubricant. The lubricant mixture was a diluted solution consisting of die lubricant, Chem Trend F-3-L and water at a ratio of 1 to 50. The specimen was rotated 90° every 3750 cycles to equalize any variation in the density of the lubricant spray on each corner. Rapid cooling from an over abundance of lubricant can have a detrimental effect on thermal fatigue resistance because it increases the temperature differential.

The surface of each specimen was examined every 5000 cycles until the test was complete at 15 000 cycles. The oxide layer which accumulated over the corners to be investigated was removed by manually polishing the specimen with a V-shaped die block utilizing 240 grit and 400 grit grinding papers. Only those cracks, which initiated along the edge of the corner and located within the central 3 inches of the specimen, were counted. The measurements were taken at a magnification of 100X with a Leitz microhardness testing unit.

The length of each crack was used to describe the thermal fatigue resistance in terms of two crack parameters. They are the average maximum crack length and the average cracked area. The average maximum crack length is the measurement of the longest crack length which initiated from the edge of the corner on each corner divided by the number of corners. This parameter is referred to by the symbol $\bar{d}$. The average cracked area is the sum of the number of cracks on each corner multiplied by the square of the crack length and divided by the number of corners. This parameter is referred to by the symbol Σnd^2. These parameters are calculated for each specimen. Both parameters are significant in determining the thermal fatigue resistance of the die because the longest crack within the die surface and the extent of cracking can be determined by the average maximum crack length and the cracked area respectively. The values of these crack parameters are indicative of the service life of the die. Figure 5 is a photograph of the area to be investigated. The dark surface is the thermal fatigue crack. The light region is the surface area of the specimen which was cracked open to expose the thermal fatigue crack. Figure 6 is a scanning electron microscope photomicrograph at 20X which compares the two exposed surfaces of the heat check corner. The right side of the photomicrograph is the surface of the thermal fatigue crack. This smooth, cleavage surface is indicative of a brittle transgranular failure. In comparison, the rougher surface on the left side of the photomicrograph contains more dimpled regions which is indicative of a ductile fracture.

Microhardness readings were taken along the diagonal of the transverse cross-section every 50 microns beginning at the edge of the corner, utilizing 500 gram load in a Leitz microhardness testing unit. The hardness measurements were taken to determine any hardening or tempering of the base material from the special surface treatments. These measurements were used to determine the relationship between the tabulated crack parameters and the microstructural changes.

DISCUSSION OF RESULTS

Thermal Fatigue Properties

The average cracked area (Σnd^2) and average maximum crack length ($\bar{d}$) parameters used to determine the heat checking resistance throughout the three

5000 cycle test intervals have been tabulated in tables III and IV for the coated and welded specimens respectively. By using these quantitative measurements, table V (a and b) was developed to arrange the specimens in order of decreasing thermal fatigue resistance. Figures 7 and 8 are plots of the average cracked area and maximum crack length, respectively. A steeper slope of the lines in figures 7 and 8 for each specimen indicates greater thermal fatigue cracking and can be used to predict initiation and propagation rates qualitatively. From the ranking of the specimens in table V and the intersection of lines in figures 7 and 8 it can be seen that the two crack parameters are independent of one another by the varying positions of the specimens throughout testing.

Table V and figures 7 and 8 at 15 000 cycles show that the stress relieved specimen demonstrated the best overall thermal fatigue resistance. The improved thermal fatigue resistance of the stress relieved specimen over the control specimen is attributed to the removal of residual stresses which were generated during the thermal cycle. Another specimen which exhibited less cracked area compared to the control and possessed superior thermal fatigue resistance with respect to all the other coatings was the Specimen with Coating A.

The bath for Coating A was composed primarily of cyanide and cyanate compounds. The treatment in the salt bath caused the diffusion of carbon and nitrogen into the H-13 die steel. Since nitrogen is more soluble than carbon in ferrous metals, it diffuses more readily into the metal. However, the carbon formed iron-carbide particles at or near the surface of the corner. These particles act as nuclei, precipitating some of the diffused nitrogen to form a tough compound zone of carbon-bearing, epsilon nitride.[6] This compound is relatively thin (≈ .005 inch) as formed in a normal 90 minute treatment. None of the brittle Fe_2N phase was formed.[6] With more nitrogen available in the bath than can be absorbed and held at the surface in the compound zone, the nitrogen begins to diffuse further into the matrix of the H-13 die steel. It should be noted that the diffusion zone is relatively limited. The increase in thermal fatigue strength is attributed to this diffusion zone, not the compressive forces created at the surface.[6]

The coating which demonstrated the worst thermal fatigue resistance was Coating E. The microstructure of the transverse cross-section of this specimen magnified at 150X can be seen in figure 9. It consists of various diffusion layers which result from the nitriding process. The nitriding process can produce a considerable amount of iron nitrides in the surface layers which results in increased hardness and can lead to surface brittleness. Apparently, the surface brittleness contributed to inferior thermal fatigue properties of this specimen. From figures 7 and 8 it can be seen that Coating E demonstrated a large amount of cracking up to 5000 cycles. However, the crack propagation rate of this specimen decreased considerably after 5000 cycles. This is probably due to the fact that the crack depths exceeded the hardened coating thickness on the surface of the specimen.

Two specimens identified as maraging steel weld I and II were tested in this investigation. The Marage I specimen contained a considerable amount of porosity, whereas the Marage II specimen was free from these defects. It is apparent from the location of the heat checks through this porosity in the Marage I welded specimen that these defects made a major contribution to the poor thermal fatigue resistance of the weld. Figure 10 is a photomicrograph taken at 45X of a gas pore located in the Marage I welded corner. Gas pores act as stress risers and the longest heat checks which occurred in this corner initiated at these defects. This behavior of the Marage I Weld is demonstrated in figures 7 and 8. The Marage II specimen was produced with a

porosity-free weld. However, the Marage II welded corner exhibited poorer thermal fatigue resistance than the Marage I welded corner. The poor thermal fatigue behavior of the Marage II Weld is attributed to the presence of considerable amounts of reverted austenite which formed in the segregated portions of the weld that have higher nickel, carbon, nitrogen, and manganese contents. This austenite formed in the 1075°-1100° F temperature range to which the specimen corners were heated during immersion. Austenite has poor thermal fatigue resistance because of its low strength, high thermal expansion, and poor thermal conductivity. The microstructure of the Marage II weld is illustrated in figure 11. This microstructure shows a background of gray colored martensite and the light regions are indicative of the segregated areas that have reverted to austenite.

The H-13 welds were all free of porosity and when tested, possessed good thermal fatigue properties. The corners welded with H-13 welding rods had thermal fatigue resistance similar to one another irrespective of its welding procedure (see table II). Because these results were so similar, the average of crack parameters were calculated after 5000, 10 000 and 15 000 cylces and plotted in figures 7 and 8. It is apparent from these figures that the average maximum crack length and crack area in these welded corners are similar to and perhaps slightly better than the control after 15 000 cycles. The good performance of these welds may be attributed to their somewhat greater hardness values over the heat treated control corners, as will be demonstrated later in this paper.

In comparing the results of the various welded H-13 corners, it appears that the post-weld heat treatment at 900° F for 3 hours performed slightly better than the post-weld heat treatment of 400° F for 3 hours. The higher temperature may have relieved more of the residual stresses in the weld before testing. Since the corners are heated to 1075°-1100° F at their highest temperature point during the thermal cycle, the effect of this post-weld treatment would be eliminated very quickly during thermal fatigue testing.

Microhardness Measurements

The microhardness readings were taken along the diagonal of the corner of the transverse metallographic specimen from the corner inward toward the base metal. The first indentation was made as close as possible to the corner edge, with the remaining readings taken at 50 micron increments. The results of the microhardness measurements on each thermal fatigue specimens are plotted in figure 12.

Significant softening of the corner with respect to the base metal is apparent to a depth of about 1200 micron along the diagonal of every specimen except the specimens with coatings D and E. The hardness of the heat treated specimen was DPH 460 or Rc 46.5 before cycling and prior to the application of the coatings. The various coating treatments significantly increased this hardness into the 60 Rockwell C range but all except the specimens with coatings D and E were softened by thermal cycling. The poorest thermal fatigue resistance (figures 7 and 8) was exhibited by specimens D and E. The poor thermal fatigue resistance of these specimens is attributed to the presence of the brittle surface layer at the corner.

Attention is also called to the generally lower hardness of the specimen that was welded with maraging steel and higher hardness of the corner of the specimen welded with the H-13 welding rod. The microhardness values of the weld and the corresponding heat-affected zones of the Marage II and H-13 welded specimens are plotted in more detail in figure 13. The welds were made

in six and ten welding passes, for the H-13 and Marage II weld, respectively. Therefore, the hardness varies for each weld depending on the thermal history of the metal. Both welds eventually reach the base H-13 steel and have a measurable, similar hardness in the 460 DPH range. However, the hardness of the maraging steel is significantly lower across nearly the entire weld area than the H-13 steel. This lower hardness results from the presence of the reverted austenite in this steel. This austenite can be formed either from the high temperature portion of the thermal fatigue cycling or from the heat affect of subsequent welding passes. The hardness of the H-13 steel weld shows considerable variation depending on location across the weld deposit. The weld metal near the corner of the thermal fatigue specimen has been softened by the thermal cycling of the test. The portion of the weld toward the base metal has been hardened by subsequent weld deposits in this multipass weld. These hardened areas have not been softened by thermal cycling because the temperatures away from the corner do not reach levels as high as that of the corners. In some cases the H-13 weld material from earlier deposits has been retempered by subsequent deposits accounting for the lower hardness. This different thermal history has produced a wide variation in hardness readings over the H-13 weld. The general hardness level is significantly higher, however, than for the Maraging II Weld. At some locations this microhardness attains high levels and the weld is undoubtedly brittle at these locations. However, no cracks were noted and this high hardness apparently did not reduce the thermal fatigue resistance. A total of six weld beads were counted in the portion of the weld which still remained; this number of weld deposits accounts for the variation in hardness values.

The stress-relieved specimen also had a somewhat higher microhardness than the control or corners with coatings A, B and C. The increased hardness of the stressed relieved specimen is caused by secondary hardening which is the result of heat treating at 1050° F for 3 hours. This treatment may also have reduced the softening in this specimen by relieving the residual stresses present. The increase in hardness may have contributed to the improved thermal fatigue resistance of the stress-relieved specimen over the coated specimens. However, the hardness value of Rc 36 is still well below the original hardness of the H-13 die steel before stress relieving.

CONCLUSIONS

The results were based on the two crack parameters called the average maximum crack length and the average cracked area. Both parameters were calculated in terms of the length of the heat checks present on the specimen surface. Each parameter is evaluated independently and is significant in determining the service life of the die. The average maximum crack length indicates the length to which a heat check has propagated within the surface. The average crack area is indicative of magnitude of cracking throughout the crack surface.

The following conclusions were reached in this investigation to determine the influence of selected surface coatings, stress-relieving and various types of welds on the thermal fatigue resistance of H-13 die steel.

1. The best thermal fatigue resistance was obtained with the specimen that was stress relieved at 1050° F after 5000 and 10 000 thermal fatigue cycles.

2. The thermal fatigue resistance of the die steel was slightly improved by coating A, which is a proprietary liquid salt cyanide treatment.

3. The ion and gas nitriding coatings D and E reduced the thermal fatigue resistance sharply while the cracking occurred within the hardened surface layer.

4. The thermal fatigue resistance of the corners produced with H-13 electrodes was generally excellent. On the average, the thermal fatigue properties of the H-13 welded specimens were slightly better than the control specimens (see figures 7 and 8). The best thermal fatigue resistance of the H-13 welded specimens was obtained when the 900° F post-weld heat treatment was employed. The higher hardness and finer structure of H-13 welds as compared to the H-13 die steel may have produced the improved thermal fatigue resistance.

5. The maraging welds were very poor in thermal fatigue resistance. In the case of the Marage I weld, considerable porosity lowered the thermal fatigue resistance. Even though the second marage weld was sound, it also possessed poorer thermal fatigue properties than the Marage I weld. The inferior thermal fatigue properties of this weld can be attributed to the partial reversion to austentite in the segregated areas. The reversion to austenite may have occurred because of the heat effect of subsequent welding passes and the high temperature portion of the thermal fatigue cycle. The presence of austenite is detrimental to the thermal fatigue resistance of H-13 die steel because of its reduced hardness, poor thermal conductivity and high thermal expansion coefficient.

REFERENCES

1. Lindberg, R. A.: Processes and Materials of Manufacture. Second ed., Allyn and Bacon, Inc., 1977, p. 294.

2. Gibbons, C. L.; Moore, A. A.; Young, R. M.: Thermal Fatigue of Die Steels: A Brief Summary and Perspective. Ind. Heat., vol. 48, no. 7, July 1981, pp. 24-29.

3. Gorbach, V. G.; Alekhin, V. G.; Kurgannova, G. L.: Determining Thermal Fatigue of Steels for Die Casting of Aluminum Alloys. Met. Sci. Heat Treat. Met., vol. 19, no. 11, Nov. 1977, pp. 982-985.

4. Wallace, J. F.: Thermal Conditions in the Die. Foundary, vol. 96, no. 10, Oct. 1968, pp. 176-179.

5. Nagy, A.: Maraging Steels for Die Casting. Met. Prog., vol. 97, no. 4, Apr. 1970, pp. 70-71.

6. Taylor, E.: Tufftride: Only Skin Deep. Met. Eng. Q., vol. 11, no. 2, May. 1971, pp. 12-16.

TABLE I. - CHEMICAL COMPOSITIONS OF H-13 DIE STEEL, H-13 WELDING ROD AND MARAGE WELDING ROD

[Compositions in weight percent.]

Element	H-13 Die steel	H-13 Welding rod	Marage rod
C	0.38	0.39	0.007
Mn	.38	.31	.04
Si	1.12	1.16	.04
Ni	--	--	18.53
Cr	5.06	5.11	--
Mo	1.26	1.50	4.84
V	.94	1.02	--
Co	--	--	7.22
Ti	--	--	.41
Al	--	--	.10
S	.008	.003	.002
P	.014	.014	.002

TABLE II. - WELD PROCEDURES AND POST-WELD HEAT TREATMENTS

Specimen	Corner	Weld material	Welding temperature, °F	Post weld treatment, °F	Time, hrs
BB	A	H-13	600	900	3
	C	H-13	RT~80	900	3
BC	B	Marage	Ambient	900	3
	D	H-13	Ambient	900	3
BD	B	H-13	Ambient	900	3
	D	Marage	Ambient	900	3
BE	B	H-13	600	400	1
	D	H-13	RT~80	400	1

TABLE III. - THERMAL FATIGUE TEST RESULTS OF H-13 DIE STEEL WITH VARIOUS DIFFUSION COATINGS

Description	Corners	Average maximum crack length: $\bar{d}(\mu \times 10^2)$			Cracked area: $\Sigma nd^2(\mu^2 \times 10^6)$		
		Number of cycles			Number of cycles		
		5000	10 000	15 000	5000	10 000	15 000
Control	A,B,C,D	1.5	7.0	19.2	0.30	6.11	42.23
Coating A	A,C	5.5	8.0	21.0	2.06	3.08	13.73
Control	B,D	8.0	12.0	20.0	14.97	26.83	53.71
Coating B	A,C	4.0	6.0	19.0	0.20	5.55	57.75
Control	B,D	3.5	10.5	22.0	1.23	24.48	73.03
Coating C	A,C	2.0	12.0	32.0	0.11	40.0	106.05
Control	B,D	7.0	8.0	22.0	16.97	28.0	54.51
Coating D	A,C	42.5	43.5	44.5	163.32	239.25	276.50
Control	B,D	3.5	10.5	22.5	0.58	10.30	37.76
Coating E	A,C	48.5	51.0	57.0	286.46	378.40	514.50
Control	B,D	2.0	6.0	15.0	0.09	18.60	44.48

TABLE IV. - THERMAL FATIGUE TEST RESULTS OF H-13 DIE STEEL WITH MARAGE WELD, H-13 WELD, AND STRESS RELIEVED CORNERS

Specimen	Corners	Description	Average maximum crack length: $\bar{d}(\mu \times 10^2)$			Cracked area: $\Sigma nd^2(\mu^2 \times 10^6)$		
			Number of cycles			Number of cycles		
			5000	10 000	15 000	5000	10 000	15 000
BB[a]	A	H-13 Weld at 600°F	5.0	8.0	11.0	8.08	16.56	24.32
	C	H-13 Weld at 80°F	4.0	5.0	9.0	3.22	11.32	15.17
	B,D	Control	3.5	4.5	7.5	2.92	5.46	24.45
BC[a]	B	H-13 Weld at RT	3.0	6.5	14.5	2.11	7.31	37.59
	D	Marage -1 at RT (avg)	20.0	33.0	64.0	15.33	47.58	135.51
	A,C	Control	3.0	7.0	15.5	2.95	6.44	40.65
BD[a]	B	H-13 Weld at RT	6.0	16.0	23.0	4.63	28.30	54.56
	D	Marage -2 at RT	12.0	47.0	79.0	20.47	120.32	258.36
	A,C	Control	8.0	11.5	15.5	11.03	33.30	46.55
BE[b]	B	H-13 Weld at 600°F	5.0	6.0	16.0	4.88	6.44	16.16
	D	H-13 Weld at RT	6.0	8.0	13.0	4.73	9.56	24.43
	A,C	Control	5.0	6.5	10.5	5.21	9.02	25.26
BI	A,B,C,D	Stress relieved	3.0	3.5	6.2	2.13	3.36	6.34
		H-13 Weld average	4.8	8.25	14.17	4.60	13.24	28.70

[a]Post Weld Treatment: 900°F for 3 hours.
[b]Post Weld Treatment: 400°F for 1 hour.

TABLE V. - THE ARRANGEMENT OF FATIGUE SPECIMENS IN ORDER OF DECREASING THERMAL FATIGUE RESISTANCE

(a) Average cracked area: Σnd^2 ($\mu^2 \times 10^6$)

5000 Cycles	10 000 Cycles	15 000 Cycles
Coating C	Coating A	Stress relieved
Coating B	Stress relieved	Coating A
Control	Coating B	H-13 Weld average
Coating A	Control	Control
Stress relieved	H-13 Weld average	Coating B
H-13 Weld average	Coating C	Coating C
Marage-1	Marage-1	Marage-1
Marage-2	Marage-2	Marage-2
Coating D	Coating D	Coating D
Coating E	Coating E	Coating E

(b) Average maximum crack length: $\bar{d}$ ($\mu \times 10^2$)

5000 Cycles	10 000 Cycles	15 000 Cycles
Control	Stress relieved	Stress relieved
Coating C	Coating B	H-13 Weld average
Stress relieved	Control	Coating B
Coating B	Coating A	Control
H-13 Weld average	H-13 Weld average	Coating A
Coating A	Coating C	Coating C
Marage-2	Marage-1	Coating D
Marage-1	Coating D	Coating E
Coating D	Marage-2	Marage-1
Coating E	Coating E	Marage-2

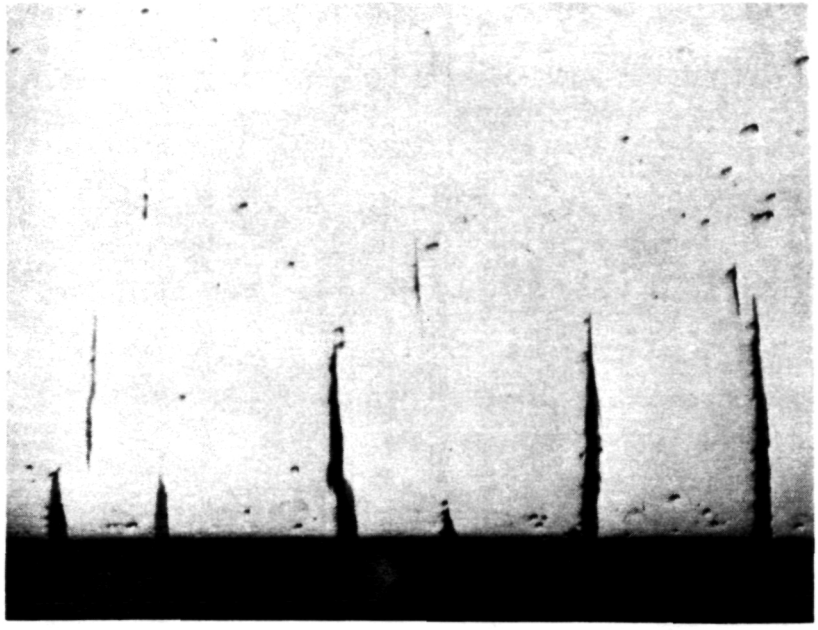

Figure 1. - The longitudinal cross-section of the control corner. Cracks initiate from the edge and propagate perpendicular to the edge of corner (Mag. 50X). No etch.

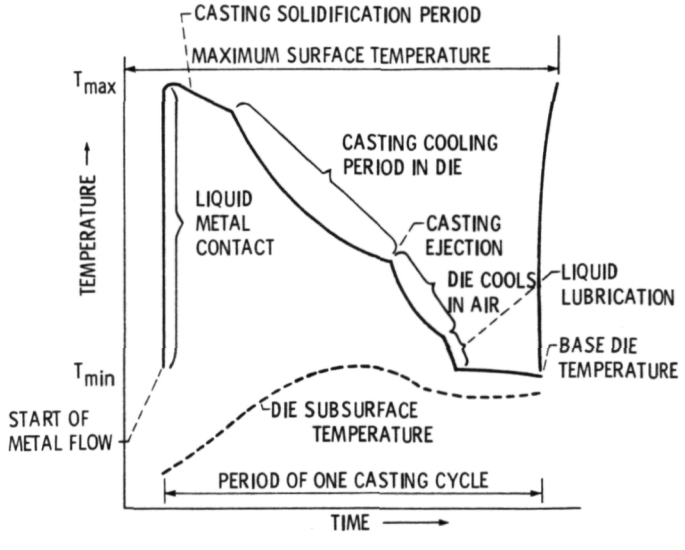

Figure 2. - An idealized temperature cycle during the die casting process.

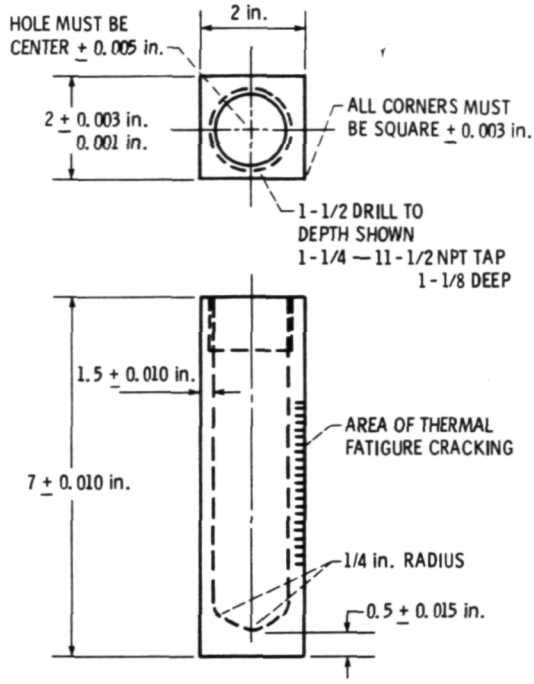

Figure 3. - Thermal fatigue specimen.

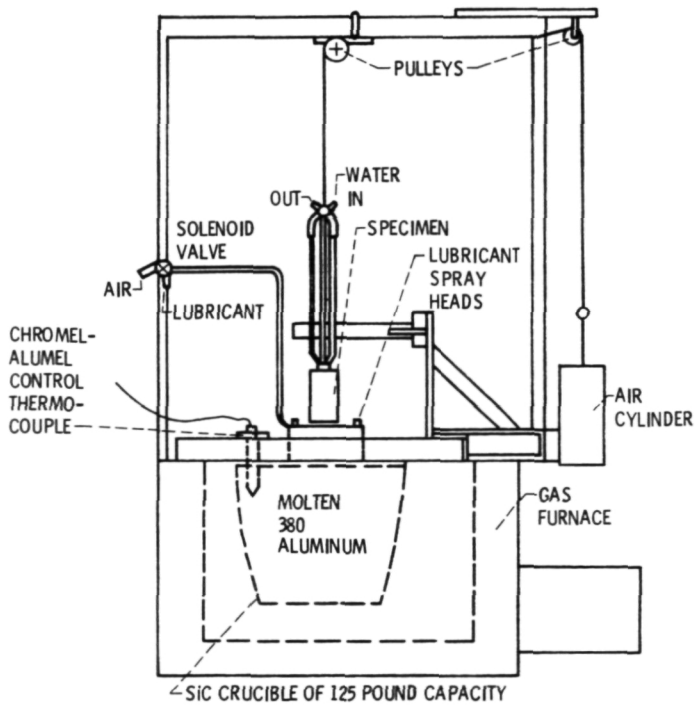

Figure 4. - Thermal fatigue test equipment.

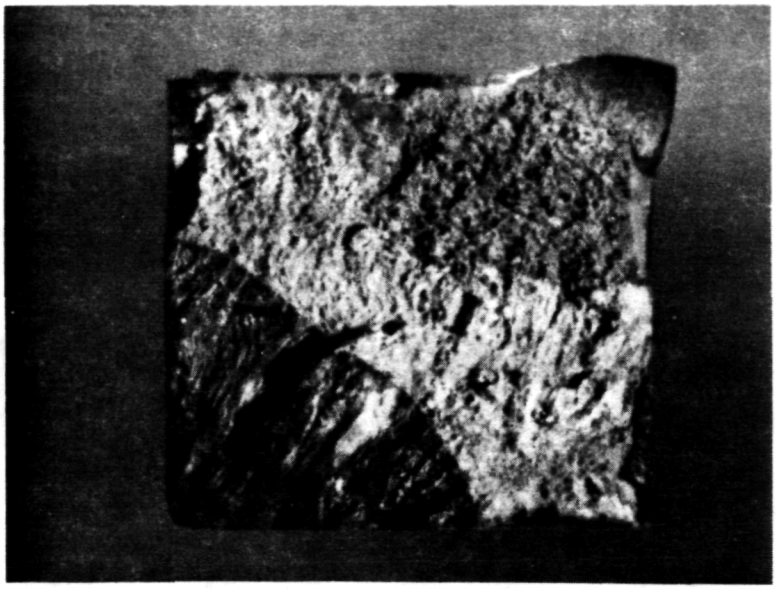

Figure 5. - The exposed surface of a heat check found in the marage II welded corner. The darkened areas is the crack and the light area is the H-13 die steel (Mag. 8X).

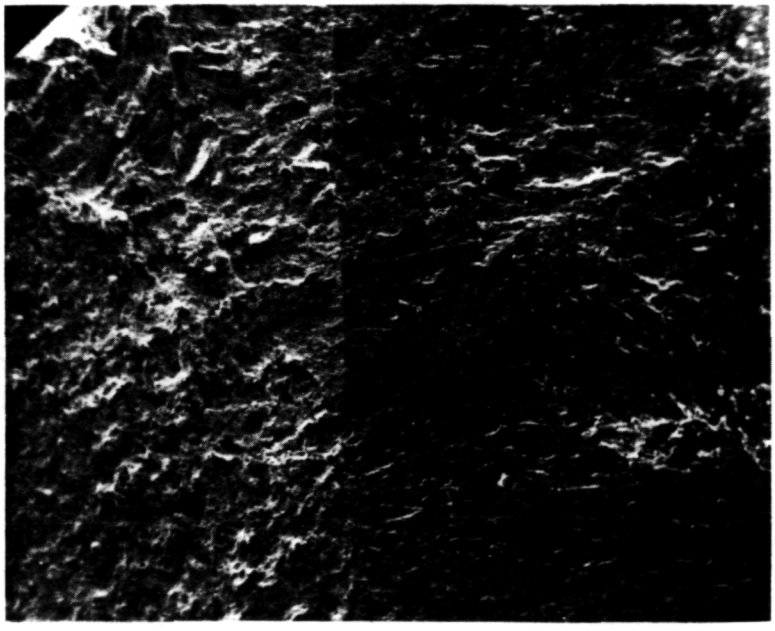

Figure 6. - The scanning electron photomicrograph of the surface of a heat check. The dark area on the right is a brittle failure associated with the thermal fatigue crack. The dimpled area on the left is the surface of the H-13 die steel exposed by mechanical failure (Mag. 20X).

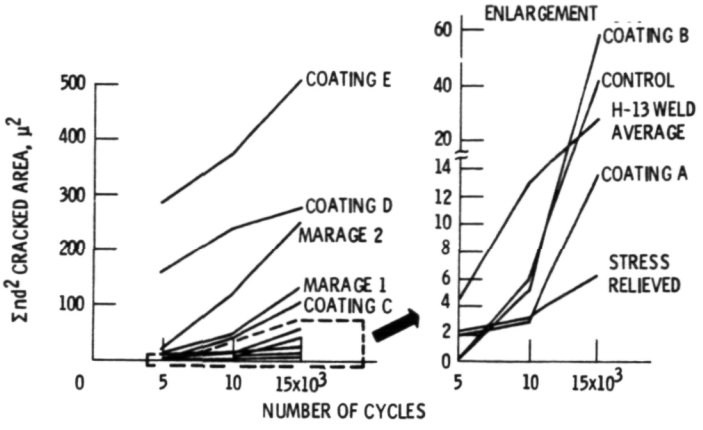

Figure 7. - Thermal fatigue test results - sums of squared cracked lengths.

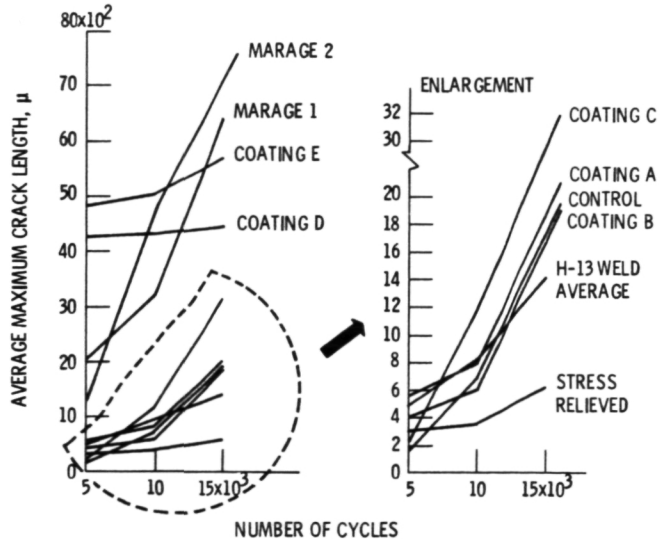

Figure 8. - Thermal fatigue test results - average maximum crack length.

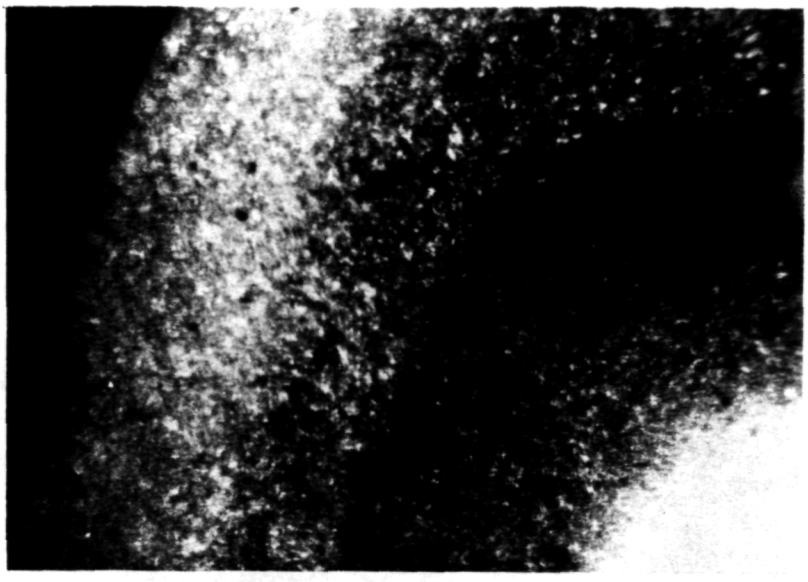

Figure 9. - The transverse cross-section of the specimen with applied coating E. It consists of various diffusion layers which resulted from the nitriding process the structure was etched by 2% nital solution (Mag. 150X).

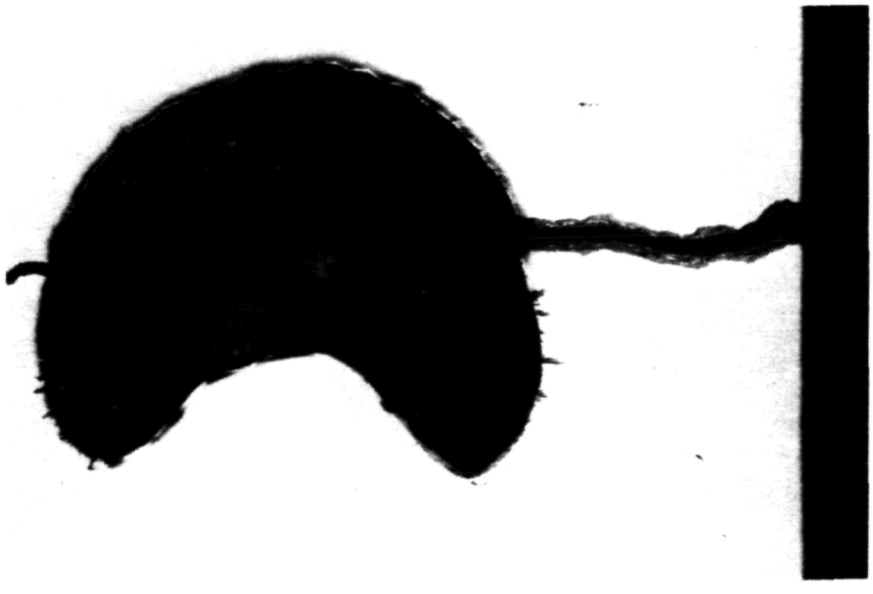

Figure 10. - The photomicrograph of a gas pore found in the marage I weld. The cavity acted as a stress riser which aided in the initiation and propagation of heat checks. No etching solution was used (Mag. 45X).

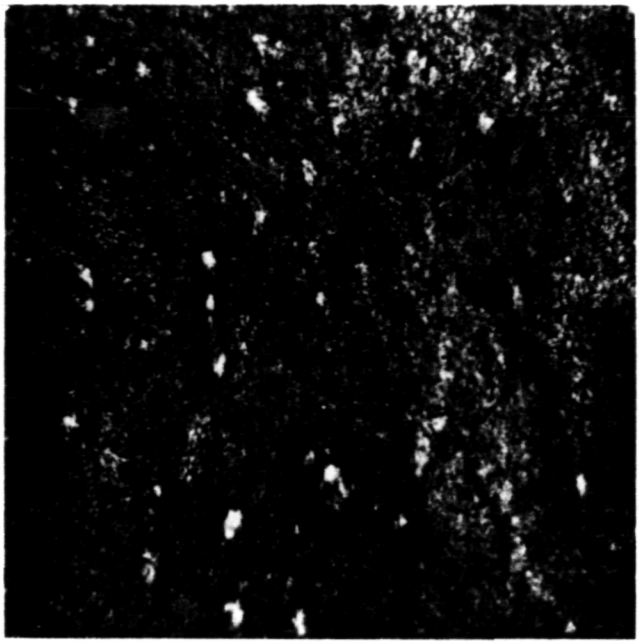

Figure 11. - The transverse cross-section of the marage II weld. Note the visible banding and segregated areas. The structure was etched with 2% nital solution (Mag. 500X).

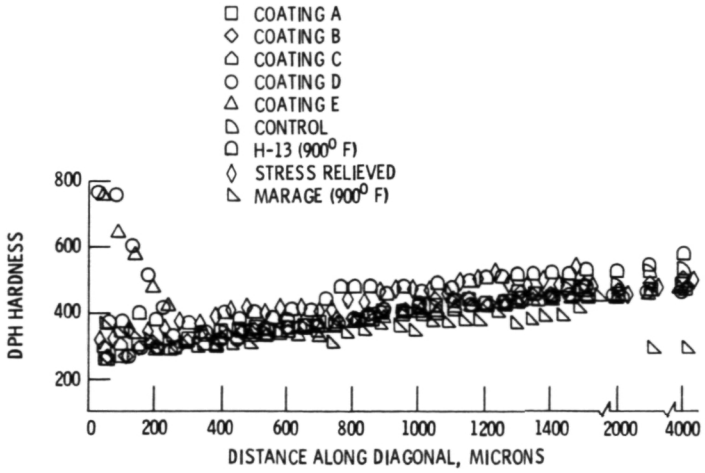

Figure 12. - DPH hardness readings along diagonal of transverse metallographic specimens.

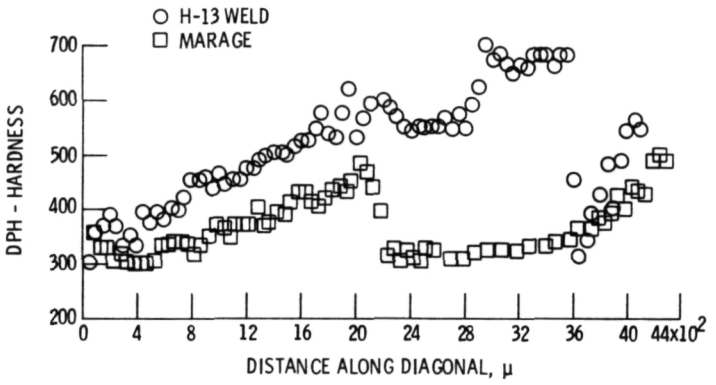

Figure 13. - DPH hardness readings along diagonal of transverse metallographic specimens to illustrate varying hardnesses throughout the heat affected zones of welded specimens.

1. Report No.	2. Government Accession No.	3. Recipient's Catalog No.
NASA TM-83331		

4. Title and Subtitle	5. Report Date
THE THERMAL FATIGUE RESISTANCE OF H-13 DIE STEEL FOR ALUMINUM DIE CASTING DIES	6. Performing Organization Code 505-33-22

7. Author(s)	8. Performing Organization Report No.
Betty J. Barrow	E-1578
	10. Work Unit No.

9. Performing Organization Name and Address	11. Contract or Grant No.
National Aeronautics and Space Administration Lewis Research Center Cleveland, Ohio 44135	
	13. Type of Report and Period Covered Technical Memorandum
12. Sponsoring Agency Name and Address National Aeronautics and Space Administration Washington, D. C. 20546	14. Sponsoring Agency Code

15. Supplementary Notes
Prepared for Let's Do It Ourselves: In Science and Technology sponsored by the National Technical Association, Baltimore, Maryland, August 2-7, 1982.

16. Abstract
This investigation was conducted to determine the effects of welding, selected surface coatings and stress relieving on the thermal fatigue resistance of H-13 Die Steel for aluminum die casting dies. Eleven thermal fatigue specimens were utilized in this investigation and are catagorized as follows: control, stress relieved, welded, and surface treated (5 different surface treatments were evaluated). Stress relieving was conducted after each 5,000 cycle interval at 1050°F for three hours. Four thermal fatigue specimens were welded with H-13 or maraging steel welding rods at ambient and elevated temperatures and subsequently, subjected to different post-weld heat treatments. The surface treatments used are proprietary but are described in generic terms. Crack patterns were examined at 5,000, 10,000, and 15,000 cycles. The thermal fatigue resistance is expressed by two crack parameters which are the average maximum crack and the average cracked area. The results indicated that a significant improvement in thermal fatigue resistance over the control was obtained from the stress-relieving treatment. Small improvements in thermal fatigue resistance were obtained from the H-13 welded specimens and from a salt bath nitrogen and carbon-surface treatment which is attributed to the alleviation of the residual stresses and the formation of a diffusion layer at the surface. The other surface treatments and welded specimens either did not affect or had a detrimental influence on the thermal fatigue properties of the H-13 die steel.

17. Key Words (Suggested by Author(s))	18. Distribution Statement
Thermal fatigue H-13 die steel Die casting dies Heat checks	Unclassified - unlimited STAR Category 26

19. Security Classif. (of this report)	20. Security Classif. (of this page)	21. No. of Pages	22. Price*
Unclassified	Unclassified		

* For sale by the National Technical Information Service, Springfield, Virginia 22161

,72'